A panchromatic modification of Metal–Organic Frameworks' light absorption spectra.

7 authors, including:

Eugenio Otal
Institute of Scientific and Technical Research…
34 PUBLICATIONS   387 CITATIONS

SEE PROFILE

Mauricio E. Calvo
Spanish National Research Council
65 PUBLICATIONS   1,026 CITATIONS

SEE PROFILE

Ismael Fabregas
National Scientific and Technical Research C…
29 PUBLICATIONS   231 CITATIONS

SEE PROFILE

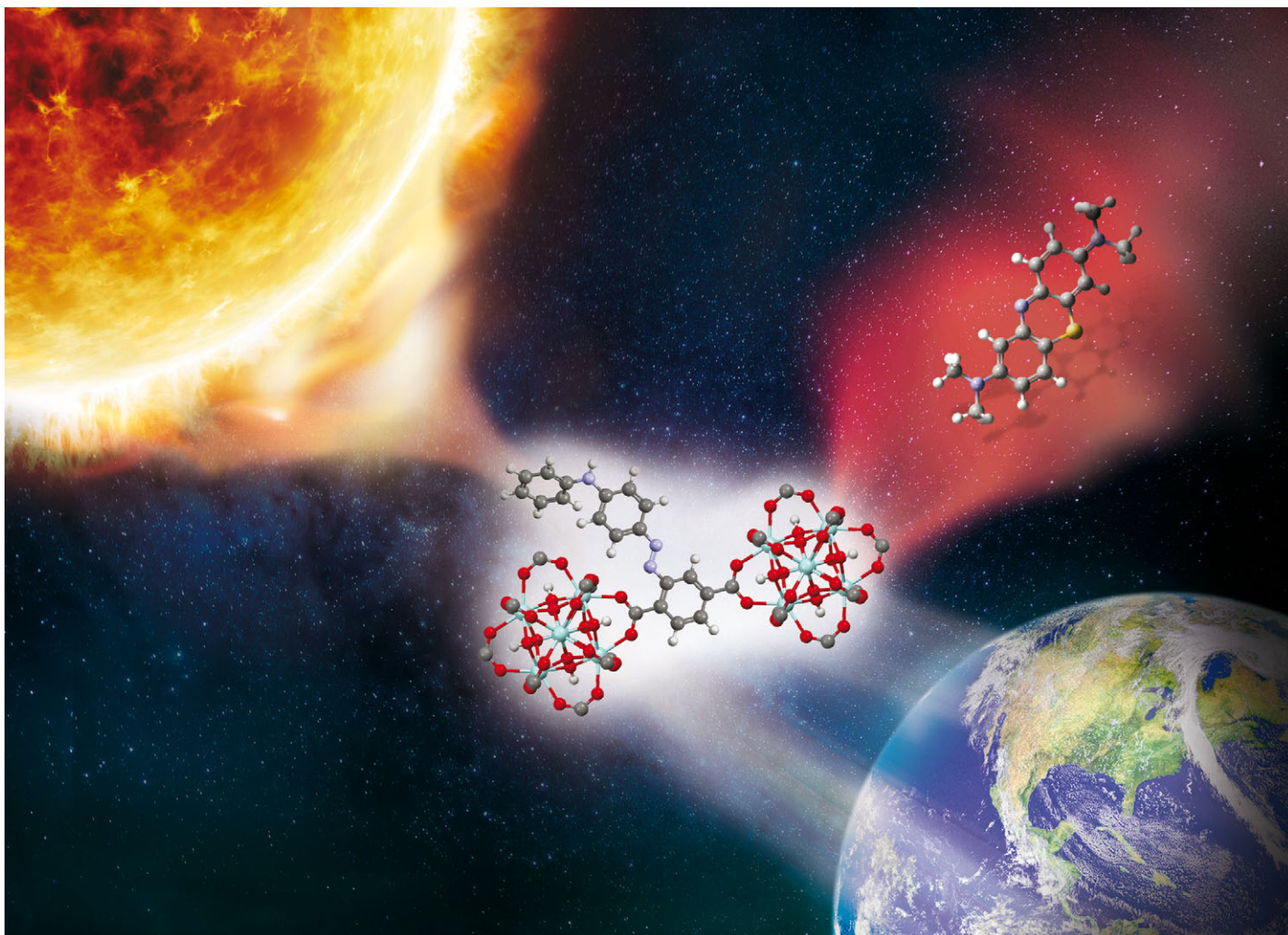**Some of the authors of this publication are also working on these related projects:**

Project SPICOLOST: "Spin, conversion, logic, storage in oxides based electronics" View project

Project Photonic Crystals View project

Showcasing research by Eugenio H. Otal **and co-workers/ UNIDEF – CONICET – CITEDEF and Laboratory for Materials Science and Technology – FRSC – UTN, Argentina.**

A panchromatic modification of the light absorption spectra of metal–organic frameworks

Dye sensitized Zr-based metal organic frameworks were obtained *via* post synthetic diazo coupling. The functionalized MOFs showed panchromatic light absorption spectra and photocatalytic performance correlated absorption edge shift. This opens up new paths to design novel photocatalytic materials.
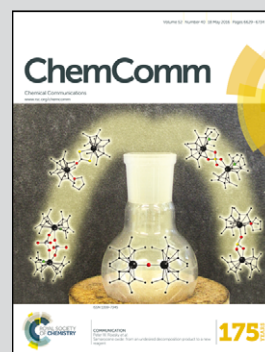
ROYAL SOCIETY
OF **CHEMISTRY**

www.rsc.org/chemcomm

ChemComm

COMMUNICATION

A panchromatic modification of the light absorption spectra of metal–organic frameworks†

E. H. Otal,*[ab] M. L. Kim,[ab] M. E. Calvo,[c] L. Karvonen,[d] I. O. Fabregas,[b] C. A. Sierra[e] and J. P. Hinestroza[f]

The optical absorption of UiO-66–NH$_2$ MOF was red-shifted using a diazo-coupling reaction. The modifications performed with naphthols and aniline yielded reddish samples, and the modifications with diphenylaniline yielded dark violet ones. The photocatalytic activity of these modified MOFs was assessed for methylene blue degradation, showing a good performance relative to traditional TiO$_2$. The degradation performance was found to correlate with the red shift of the absorption edge. These findings suggest potential applications of these materials in photocatalysis and in dye sensitized solar cells.

Metal–organic frameworks (MOFs) are coordination polymers with a high surface area.[1] These supramolecular coordination complexes have rigid organic bridges linked to clusters of metal oxides coordinated through different groups like hydroxyl, oxo, carboxylate, *etc.* The chemical and physical properties of MOFs can be tuned by a judicious selection of the linker, the metal-oxide centre and the pore size.

One of the most studied frameworks is MOF 5,[2] a MOF with a periodic arrangement of Zn$_4$O clusters as secondary building units (SBUs) linked by terephthalate ions. This array of SBUs has a crystalline order that can be defined as a three-dimensional periodic pattern of II–VI semiconductor nanoparticles. However, unlike II–VI semiconductor nanoparticles prepared *via* chemical routes, where surface coordination and particle size distribution vary, in MOFs the number of atoms, coordination and distance in each Zn$_4$O cluster are crystallographically well defined.

MOFs can also behave as semiconductors.[3,4] The use of semiconductor nanoparticles in photocatalytic applications has the drawback of a potential reduction of the surface area due to the agglomeration of the nanoparticles. Additionally, their large band-gap energy leads mostly to absorption in the UV range of the electromagnetic spectrum. When MOFs are used, the first problem can be neglected due to the inherent high surface area of MOFs (>1000 m^2 g^{-1}) and the large number of highly accessible pores.

In semiconductors, the problem of shifting the absorption spectra to the visible range to improve light harvesting was solved by Grätzel *et al.*[5,6] Their approach was based on the adsorption of a ruthenium complex dye at the surface of TiO$_2$ nanoparticles. This system opened a large new field in photovoltaics known as dye sensitized solar cells (DSSCs). Recently, the use of a new family of metal-free dyes has allowed the replacement of ruthenium complexes in DSSCs.[7,8] These new systems are composed of an electron donor group (*e.g.* triphenyl-amine) bridged through a π-system (C=C or N=N) to an acceptor group (*e.g.* cyanoacrylic acid). The acceptor–π–donor system (A–π–D) is attached to the semiconductor, typically TiO$_2$, through a carboxylic group.

This strategy can be also used to sensitize MOFs, through the introduction of different dyes as organic linkers, and thus, extend their spectral absorption to the visible range for the resulting material. One way to do so includes post-synthetic modifications of a synthon introduced as an organic linker into the MOF structure. This strategy was reported earlier by Burrows *et al.* who used an aldehyde-synthon as a linker on a Zn-based MOF for its later transformation into a hydrazone.[9] Similarly, nitrogen functional groups can be also used, taking advantage of their chemical versatility which allows for more flexibility than aldehydes. Jiang *et al.* performed a tandem diazotization reaction

[a] Laboratory for Materials Science and Technology, FRSC-UTN, Av. Inmigrantes 555, Río Gallegos 9400, Argentina

[b] Division of Porous Materials, UNIDEF, CITEDEF, CONICET, S. J. B de la Salle 4397, Villa Martelli (B1603ALO), Buenos Aires, Argentina. E-mail: eotal@citedef.gob.ar

[c] Instituto de Ciencia de Materiales de Sevilla (Consejo Superior de Investigaciones Científicas-Universidad de Sevilla), C/Américo Vespucio 49, 41092 Sevilla, Spain

[d] Solid State Chemistry and Catalysis, Empa – Swiss Federal Laboratories for Materials Science and Technology, Überlandstrasse 129, CH-8600 Dübendorf, Switzerland

[e] Department of Chemistry, Faculty of Sciences, Universidad Nacional de Colombia, Bogotá, Colombia

[f] Laboratory of Textiles and Nanotechnology, Department of Fiber Science and Apparel Design, Cornell University, Ithaca, New York, USA

† Electronic supplementary information (ESI) available: Synthesis description, characterization details, photographs of powders, schemes of MOFs and TGA calculations. See DOI: 10.1039/c6cc02319c

on MIL-101–Cr–NH$_2$ to introduce halo, hydroxyl and azo groups,[10] Nasalevich *et al.* performed a diazo coupling to increase the visible light absorption range and improve the photocatalytic performance on MIL-125(Ti)–NH$_2$,[11] and Aguilera-Sigalat and Bradshaw modified UiO-66–NH$_2$ for fluorescence based pH sensors.[12] In our case, we use UiO-66–NH$_2$, a Zr-based MOF where the SBU is Zr$_6$O$_4$(OH)$_4$ that enables exceptional stability in water.[13,14] This enhanced water stability allows us to generate materials for photocatalytic applications in different environments and targets.

The diazo coupling reactions of UiO-66–NH$_2$ with *N,N*-dimethylaniline, 1-naphthol, 2-naphthol and diphenylamine yielded strongly coloured solids. Diazo coupling was not successful when cresyl blue, basic fuchsin, malachite green, or crystal violet was used. The failure of the reaction with these compounds was presumably due to the similar size of these molecules to the pore size of the MOF, both around 1 nm. The coupling of these molecules with the amino groups closer to the external surface may also block the access of the reactant to the inner pores preventing their diffusion through the porous network. No diazo coupling was achieved when UiO-66 was testesd as the starting material.

In order to analyse the structural changes after the diazo coupling, we show in Fig. 1 the XRD patterns for all diazo coupled MOF powders. For the sake of comparison, all diffractograms were normalized to the (111) peak. In all cases, the samples exhibit the UiO-66 diffraction pattern with no extra phases but with differences in the intensities of some peaks. The differences are attributed to the introduction of rigid (but not static) organic groups that change the electronic density in certain planes of the UiO-66 crystalline structure. The most remarkable of these differences is observed in the (600) reflection that corresponds to a plane where the diazo group and part of the rigid organic chain are located. Also the intensity ratio of peaks (331)/(420) shows some variation. In UiO-66–NH$_2$, these two peaks exhibit a similar intensity, but in the rest of the samples, the (331) reflection is more intense. The reason for this asymmetry is that the plane (331) crosses the aromatic rings of the terephthalate linkers across Carbon-2 and Carbon-5, where

Table 1   Specific surface area, energy gap from Tauc plot and methylene blue degradation performance

Sample	Specific surface area[a] (m^2 g^{-1})	Energy gap (eV)	Methylene blue degradation (%)
TiO$_2$	45	3.25	100
UiO-66	563	3.70	42
UiO-66–NH$_2$	566	2.87	63
N,N-Dimethylaniline	816	1.89	75
1-Naphthol	364	1.94	58
2-Naphthol	359	2.00	4
Diphenylamine	451	1.71	91

[a] Calculated from BET theory.

the amino group is attached, hence increasing the electronic density in the post-functionalized solids. In the second case, plane (420) crosses the terephthalate across a specular plane that does not include any carbon from the aromatic ring, hence keeping a constant electronic density when performing the functionalization (see the ESI†).

To obtain information of the specific surface area in the modified MOFs, nitrogen sorption measurements were performed (see the ESI†). All isotherms exhibited type I behaviour, in agreement with previous reports for UiO-66.[15] Type I isotherms indicate microporous powders with a pore diameter size in the range of a few molecular nitrogen diameters. From these data we can estimate the specific surface area (SSA) for all the solids (Table 1). All samples exhibited a low SSA with respect to those previously reported in the literature ($\sim$1400 m^2 g^{-1}).[16] This observation can be assigned to the sensitivity of the SSA under the synthesis conditions. Interestingly, the *N,N*-dimethylaniline coupled sample exhibited a higher SSA than the uncoupled one. This lack of correlation of SSA with the coupled organic side chain volume was previously observed in functionalized samples *via* amide formation with different acid anhydrides.[17]

In order to analyse the solvent content, the approximate diazo coupling yield, and the average molar mass, a thermogravimetric analysis coupled to mass spectrometry (TGA-MS) of all the samples was performed. From the analysis of these results, we detected a first mass loss step attributed to water occluded in the pores, as shown by the m/z = 18 peak (see the ESI†). The CO$_2$ peak (m/z = 44) was not observed up to 450 °C in the UiO-66 sample, while the rest of the samples exhibited a CO$_2$ signal at around 350 °C. The diphenylamine sample showed a complex decomposition path and its CO$_2$ peak appeared at 250 °C. Even though diazo coupled samples have a high thermal stability, the structure modification made them less stable than the unmodified UiO-66.

The yield of the diazo coupling was roughly estimated from TGA-MS mass loss measurements. This estimation is based on the hypothesis that the mass losses correspond to solvent elimination and transformation of the organic part of the MOFs into combustion products and ZrO$_2$. Also, we speculate that the molecular mass of this organic part is composed by successfully diazo-coupled MOF and UiO-66–OH (a product of diazonium salt decomposition). The values for a yield percentage of the diazo coupling reaction and a more detailed discussion are
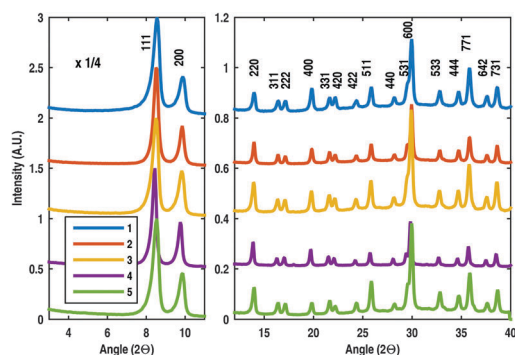

Fig. 1   X-Ray diffraction patterns for samples with and without diazo coupling reaction; left side reflection intensities are divided by four. Sample IDs: (1) UiO-66–NH$_2$ (blue line), (2) *N,N*-dimethylaniline (red line), (3) 1-naphthol (yellow line), (4) 2-naphthol (violet line), and (5) diphenylamine (green line).

presented in the ESI.† In all cases the yield of the diazo coupling was estimated below 25%, and similar yields were obtained for functionalization *via* amide formation.[17] This fact could be explained considering that the reactants diffuse through the pore; they may find several diazonium ion groups (the nucleophilic reaction has a high efficiency, as N_2 is an excellent leaving group), and the coupling reaction will occur, making the reaction more likely to occur on the sites closest to the surface. Once the coupling reaction occurs, the pore size is reduced, hence decreasing diffusion through the pores. As a consequence, an unreacted core and a shell of functionalized MOF are formed. The molecules that failed to react (cresyl blue, basic fuchsin, malachite green and crystal violet) are drastic cases of surface pore blocking, shielding the internal part of the MOF and impeding the continuation of the reaction.

Raman spectroscopy was used to determine the tautomeric configuration of modified linkers. Tautomeric equilibrium is related to the proton transfer among two or more functional groups in a molecule with a direct impact on the electronic density and, consequently, on the absorption spectra. In the case of modified MOFs, this equilibrium can be present and can be strongly influenced by temperature, solvent polarity, pH and electron withdrawing substituents.[18] Vibrational spectroscopies are a very precise tool to identify the predominant species in this tautomeric equilibrium. In the case of infrared spectroscopy (FTIR), only the disappearance of the amino groups in the modified samples was clearly observed (see the ESI†). While Raman spectroscopy showed that samples coupled with *N,N*-dimethylaniline and diphenylamine are protonated and the azo-quinonoid equilibrium is displaced to the quinonoid-form due to the use of acetic acid and acetone during the washing step of the samples. The use of a polar solvent and an acid shifts the equilibrium to the quinonoid form and increases the visible light absorption range[19] (see the ESI†). In samples coupled with *N,N*-dimethylaniline, the increase of pH transformed the sample from deep red to yellow; this can be explained by their similar structures to methyl orange, which also change their colour from red to yellow. In the case of the diphenylamine coupled sample, similar behaviour was observed for pH, changing the colour of the samples from deep violet to light yellow. Samples coupled with naphthols are in an azo-hydrazone tautomeric equilibrium but independent of pH; they are only influenced by the polarity of the solvent used for washing the samples, acetic acid and acetone (see the ESI† for Raman spectra and chemical species involved in the equilibrium).

The diazo-coupled reaction allows us to extend the absorption range of the unmodified MOF. After the reaction, we obtained a colour palette indicating that the diazo coupling was successful (see the ESI†). In order to determine the absorption band-gap, diffuse reflectance spectra of all specimens were measured (Fig. 2). The UiO-66 sample presents no absorption in the whole visible range, while UiO-66–NH_2 shows a shoulder at 400 nm, which disappears at 450 nm. The samples coupled with 1-naphthol and 2-naphthol exhibit similar spectra and a maximum absorption peak at 500 nm with a tail up to 600 nm.
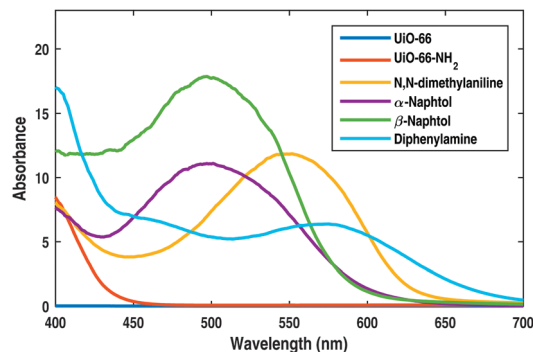

Fig. 2 Diffuse reflectance spectra for UiO-66, UiO-66–NH_2 and UiO-66–NH_2 diazo coupled samples. The UiO-66 sample (blue line) does not exhibit light absorbance in the reported range.
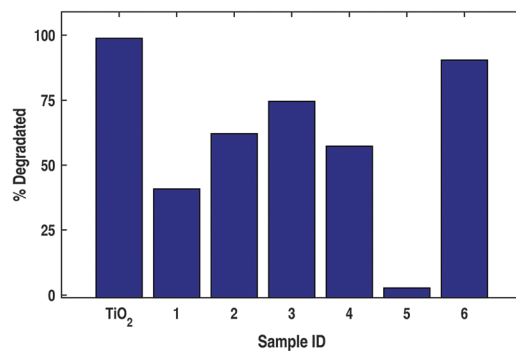

Fig. 3 Photocatalytic performance of coupled and uncoupled samples with respect to TiO_2. Sample IDs: (1) UiO-66, (2) UiO-66–NH_2, (3) *N,N*-dimethylaniline, (4) 1-naphthol, (5) 2-naphthol, and (6) diphenylamine.

The *N,N*-dimethylaniline sample has even more extended spectra, but with the maximum absorption peak at 550 nm. The diphenylamine modified sample has a panchromatic coverage of the visible spectra, with a broad constant absorption peak up to 700 nm. The red shift of the absorption spectra is in agreement with predictions from the particle in a box model; longer boxes indicate a larger red shift in the absorption spectra.

To better show the red shift in the absorption spectra, the data were transformed into Tauc plots assuming direct allowed transitions (Table 1). The results of the transformation indicate that the absorption onset of the diphenylamine modified MOF is close to the minimum band gap for successful water splitting at pH = 0, 1.23 eV.

One direct and simple test of photocatalytic activity is the degradation of pollutants.[20] Nasalevich *et al.* showed the oxidation of benzaldehyde with a diazo modified MIL-125(Ti)–NH_2,[11] while Wang *et al.*[21] and Liang *et al.*[22] tested the performance on Cr(IV) reduction with MIL-125(Ti) and MIL-68(In)–NH_2, respectively. Laurier *et al.* observed the degradation of organic dyes, rhodamine 6G, with Fe-based MOFs.[23] In our case, to prove the photocatalytic properties of the solids, the degradation of methylene blue in aqueous solution was performed (see Fig. 3 and ESI† for experimental details). The degradation performance is correlated with the shift in the absorption edge of the MOFs (Fig. S6, ESI†).

The only disagreement with this tendency is found in 1-naphthol and 2-naphthol coupled samples, and this observation can be due to their low specific area (see Table 1).

This work reports on the successful modification of the absorption spectrum of UiO-66 MOF by covalent modification covering the whole visible spectrum. Covalent modification was performed *via* a diazo coupling of MOFs with amino substituted ligands and other molecules of limited size. It was observed that molecules with more than two aromatic rings did not react successfully under MOF-postfunctionalization conditions due to pore size exclusion. Diffusion through the pores was reduced by the functionalization, leaving a core of unreacted MOF coated with a functionalized shell. The covalent modification left the structure intact, maintaining its XRD pattern. This work shows that a judicious selection of coupling molecules produces significant modifications in the absorption spectra and that panchromaticity can be achieved. The promising photocatalytic properties shown in pollutant degradation suggest the potential application of these materials in the field of dye sensitized solar cells and water splitting.

Notes and references

1 M. O'Keeffe and O. M. Yaghi, *Chem. Rev.*, 2012, **112**, 675–702.
2 S. S. Kaye, A. Dailly, O. M. Yaghi and J. R. Long, *J. Am. Chem. Soc.*, 2007, **129**, 14176–14177.
3 C. G. Silva, A. Corma and H. García, *J. Mater. Chem.*, 2010, **20**, 3141.
4 M. Alvaro, E. Carbonell, B. Ferrer, F. X. Llabrés i Xamena and H. Garcia, *Chem. – Eur. J.*, 2007, **13**, 5106–5112.
5 B. O'Regan and M. Grätzel, *Nature*, 1991, **353**, 737–740.
6 J.-H. Yum, E. Baranoff, S. Wenger, M. K. Nazeeruddin and M. Grätzel, *Energy Environ. Sci.*, 2011, **4**, 842–857.
7 D. P. Hagberg, T. Edvinsson, T. Marinado, G. Boschloo, A. Hagfeldt and L. Sun, *Chem. Commun.*, 2006, 2245–2247.
8 A. Mishra, M. K. R. Fischer and P. Bäuerle, *Angew. Chem., Int. Ed. Engl.*, 2009, **48**, 2474–2499.
9 A. D. Burrows, C. G. Frost, M. F. Mahon and C. Richardson, *Angew. Chem., Int. Ed. Engl.*, 2008, **47**(44), 8482–8486.
10 D. Jiang, L. L. Keenan, A. D. Burrows and K. J. Edler, *Chem. Commun.*, 2012, **48**, 12053–12055.
11 M. A. Nasalevich, M. G. Goesten, T. J. Savenije, F. Kapteijn and J. Gascon, *Chem. Commun.*, 2013, **49**, 10575–10577.
12 J. Aguilera-Sigalat and D. Bradshaw, *Chem. Commun.*, 2014, **50**, 4711–4713.
13 J. H. Cavka, S. Jakobsen, U. Olsbye, N. Guillou, C. Lamberti, S. Bordiga and K. P. Lillerud, *J. Am. Chem. Soc.*, 2008, **130**, 13850–13851.
14 S. Jakobsen, D. Gianolio, D. S. Wragg, M. H. Nilsen, H. Emerich, S. Bordiga, C. Lamberti, U. Olsbye, M. Tilset and K. P. Lillerud, *Phys. Rev. B: Condens. Matter Mater. Phys.*, 2012, **86**, 125429.
15 S. Chavan, J. G. Vitillo, D. Gianolio, O. Zavorotynska, B. Civalleri, S. Jakobsen, M. H. Nilsen, L. Valenzano, C. Lamberti, K. P. Lillerud and S. Bordiga, *Phys. Chem. Chem. Phys.*, 2012, **14**, 1614–1626.
16 A. Schaate, P. Roy, A. Godt, J. Lippke, F. Waltz, M. Wiebcke and P. Behrens, *Chem. – Eur. J.*, 2011, **24**, 6643–6651.
17 M. Kandiah, S. Usseglio, S. Svelle, U. Olsbye, K. P. Lillerud and M. Tilset, *J. Mater. Chem.*, 2010, **20**, 9848–9851.
18 M. A. Rauf, S. Hisaindee and N. Saleh, *RSC Adv.*, 2015, **5**, 18097–18110.
19 A. G. Gilani, M. Moghadam, M. S. Zakerhamidi and E. Moradi, *Dyes Pigm.*, 2011, **91**(2), 170–176.
20 C. C. Wang, J. R. Li, X. L. Lv, Y. Q. Zhang and G. Guo, *Energy Environ. Sci.*, 2014, **7**, 2831–2867.
21 H. Wang, X. Yuan, Y. Wu, G. Zeng, X. Chen, L. Leng, Z. Wu, L. Jiang and H. Li, *J. Hazard. Mater.*, 2015, **286**, 187–194.
22 R. Liang, J. Shen, F. Jing and L. Wu, *Appl. Catal., B*, 2015, **162**, 245–251.
23 K. G. M. Laurier, F. Vermoortele, R. Ameloot, D. E. De Vos, J. Hofkens and M. B. J. Roeffaers, *J. Am. Chem. Soc.*, 2013, **135**(39), 14488–14491.